DOI 10.1002/mnfr.200800245 Mol. Nutr. Food Res. 2009, *53*, 726 – 738

Research Article

Bog blueberry anthocyanins alleviate photoaging in ultraviolet-B irradiation-induced human dermal fibroblasts

Ji-Young Bae[1], Soon Sung Lim[1], Sun Ju Kim[2], Jung-Suk Choi[1], Jinseu Park[3], Sung Mi Ju[3], Seoung Jun Han[4], Il-Jun Kang[1] and Young-Hee Kang[1]

[1] Department of Food and Nutrition and Korean Institute of Nutrition, Hallym University, Chuncheon, Republic of Korea
[2] Institute of Natural Medicine, Hallym University, Chuncheon, Republic of Korea
[3] Department of Biomedical Science, Hallym University, Chuncheon, Republic of Korea
[4] Seorim Bio Co., Hupyung-dong, Chuncheon, Republic of Korea

Fruits of bog blueberry (*Vaccinium uliginosum* L.) are rich in anthocyanins that contribute pigmentation. Anthocyanins have received much attention as agents with potentials preventing chronic diseases. This study investigated the capacity of anthocyanin-rich extract from bog blueberry (ATH-BBe) to inhibit photoaging in UV-B-irradiated human dermal fibroblasts. BBe anthocyanins were detected as cyanidin-3-glucoside, petunidin-3-glucoside, malvidin-3-glucoside, and delphinidin3-glucoside. ATH-BBe attenuated UV-B-induced toxicity accompanying reactive oxygen species (ROS) production and the resultant DNA damage responsible for activation of p53 and Bad. Preincubation of ATH-BBe markedly suppressed collagen degradation *via* blunting production of collagenolytic matrix metalloproteinases (MMP). Additionally, ATH-BBe enhanced UV-B-downregulated procollagen expression at transcriptional levels. We next attempted to explore whether ATH-BBe mitigated the MMP-promoted collagen degradation through blocking nuclear factor κB (NF-κB) activation and MAPK-signaling cascades. UV-B radiation enhanced nuclear translocation of NF-κB, which was reversed by treatment with ATH-BBe. The UV-B irradiation rapidly activated apoptosis signal-regulating kinase-1 (ASK-1)-signaling cascades of JNK and p38 mitogen-activated protein kinase (p38 MAPK), whereas ATH-BBe hampered phosphorylation of c-Jun, p53, and signal transducers and activators of transcription-1 (STAT-1) linked to these MAPK signaling pathways. ATH-BBe diminished UV-B augmented-release of inflammatory interleukin (IL)-6 and IL-8. These results demonstrate that ATH-BBe dampens UV-B-triggered collagen destruction and inflammatory responses through modulating NF-κB-responsive and MAPK-dependent pathways. Therefore, anthocyanins from edible bog blueberry may be protective against UV-induced skin photoaging.

Keywords: Anthocyanin-rich bog blueberry / Human dermal fibroblasts / Matrix metalloproteinase / Photoaging / Ultraviolet-B

Received: June 21, 2008; revised: July 26, 2008; accepted: August 2, 2008

1 Introduction

Human skin is directly exposed to environmental factors such as UV radiation from the sun [1], which is one of the most ubiquitous damaging environmental impacts [2, 3]. UV radiation is responsible as a causative factor for various skin lesions including photoaging and photocarcinogenesis [4, 5]. UV radiation is known to alter cellular function *via*

Correspondence: Dr. Young-Hee Kang, Department of Food and Nutrition, Hallym University, Chuncheon, Kangwon-do 200-702, Republic of Korea
E-mail: yhkang@hallym.ac.kr
Fax: +82-33-254-1475

Abbreviations: ASK-1, apoptosis signal-regulating kinase-1; **ATH-BBe,** anthocyanin-rich bog blueberry extract; **ATR,** ataxia telangiectasia and rad3-related kinase; **DCHF-DA,** 2′,7′-dichlorodihydrofluorescein diacetate; **DMEM,** dulbecco's modified eagle's media; **ECM,** extracellular matrix; **EGCG,** epigallocatechin-3-gallate; **FBS,** fetal bovine serum; **GAPDH,** glyceraldehyde-3-phosphate dehydrogenase; **IL,** interleukin; **MMP,** matrix metalloproteinase; **MTT,** 3-(4,5-dimetylthiazol-yl)-diphenyl tetrazolium bromide; **NF-kB,** nuclear factorkB; **p38 MAPK,** p38 mitogen-activated protein kinase; **ROS,** reactive oxygen species; **RT-PCR,** reverse-transcriptase polymerase chain reaction; **STAT-1,** signal transducers and activators of transcription-1

DNA damage and inflammatory responses [4, 6, 7]. In addition, damage to the extracellular matrix (ECM) integrity in skin tissues is an important event entailing skin wrinkle and blister formation, hallmarks of photoaging [7, 8]. UV-induced ECM alterations observed in premature skin aging and in aged skin are considered as the result of the production of various matrix metalloproteinases (MMP) by cutaneous cells [7, 9]. Human skin expresses various collagenolytic MMP including MMP-1, MMP-8, and MMP-13, all of which attack native fibrillar collagen and elastin responsible for the strength and resiliency of skin [7]. Accordingly, the fibril disarrangement during photoaging causes the skin to appear aged [8]. Inhibition of MMP expression and activity is one of the strategies to prevent UV-initiated photodamage caused by a complex cascade of biochemical reactions in human skin.

There is substantial evidence for underlying mechanisms of human skin photoaging. UV radiation causes generation of reactive oxygen species (ROS) and resultant alterations in complex signaling events [10, 11]. In addition, UV irradiation-triggered oxidative stress regulates a variety of cellular functions including collagen fragmentation and MMP secretion [12]. It was proposed that antioxidants scavenging and quenching ROS can prevent skin photoaging. Antioxidant N-acetyl cysteine inhibited UV-induced human skin aging through mitogen-activated protein kinase (MAPK) signaling pathways [11]. In our previous study, epigallocatechin gallate (EGCG) mitigated UV-B radiation-induced oxidative stress and activation of signaling pathways in human dermal fibroblasts [12]. Furthermore, UV causes increased synthesis and release of proinflammatory mediators from a variety of skin cells [7]. These mediators increase infiltration and activation of neutrophils and other phagocytic cells into the skin, resulting in further inflammation and MMP activation. Blockade of inflammation using inhibitors of cyclooxygenase and cytokine generation might be an approach for the treatment of skin aging initiated by UV [13]. The inflammation activates various matrices-degrading MMP, leading to abnormal matrix degradation and accumulation of nonfunctional matrix components [14].

Previous studies showed that polyphenols can be promising agents reducing the risk of skin diseases [15 – 17]. Intensive interest has been focusing on the beneficial dermal effects of dietary polyphenols due to their antioxidative and anti-inflammatory activities in the skin [11, 18]. Silymarin inhibited UV-induced oxidative stress in both epidermal and dermal cells through targeting infiltrating the skin CD11b + cells [19]. In addition, polyphenol-rich plant extracts are effective in dampening the oxidative cellular damage of UV radiation and preventing skin cancer cell proliferation [20, 21]. Administration of dietary grape seed proanthocyanidins is effective in inhibiting and lightening UV-B-induced photocarcinogenesis and pigmentation in animal skin models [22, 23]. However, inhibitory actions of bog blueberry polyphenols in the photoaging are not well defined. Considering that plant pigment proanthocyanidin inhibits UV-B-induced oxidative stress in mice [22], it was hypothesized that anthocyanin-related redox manipulations block UV photoaging and skin inflammation by influencing the MAPK signaling pathways.

To test this hypothesis, the current study elucidated the mechanisms of action of anthocyanin-rich extract from edible bog blueberry (ATH-BBe) by downregulating mid-wave UV-B (280 – 320 nm) irradiation-induced collagen degradation and inflammatory mediator production in human dermal fibroblasts. UV-B is one of the most important external stimuli that affects skin by inducing immunosuppression, cancer, premature skin aging, inflammation, and cell death. We tested whether ATH-BBe manipulates collagenolytic MMP production *via* modulating NF-κB-responsive and MAPK- dependent pathways that converge at the level of transcriptional regulation in UV-B-exposed human dermal fibroblasts.

2 Materials and methods

2.1 Materials

Human dermal fibroblasts were obtained from Clonetics (San Diego, CA). Dulbecco's modified eagle's media (DMEM) and culture reagents were purchased from Sigma – Aldrich Chemicals (St. Louis, MO). Fetal bovine serum (FBS), penicillin – streptomycin, and trypsin – EDTA were provided from Lonza (Walkersville, MD). 3-(4,5-Dimetylthiazol-yl)-diphenyl tetrazolium bromide (MTT) and 2′,7′-dichlorodihydrofluorescein diacetate (DCHF-DA) were obtained from DUCHEFA Biochemie (Haarlem, The Netherlands) and Sigma – Aldrich Chemicals, respectively. Antibodies against human MMP-1, human MMP-8, human MMP-13, human type1 collagen, human type1 procollagen, and human nuclear factorκB (NF-κB) were obtained from Santa Cruz Biotechnology (Santa Cruz, CA). Antibodies against phospho-apoptosis signal-regulating kinase-1 (ASK-1), phospho-c-Jun N-terminal kinase (JNK), phospho-p38 mitogen-activated protein kinase (p38 MAPK), phospho-c-Jun, phospho-p53, inhibitory κB (IκB), phospho-IκB, phospho-signal transducers and activators of transcription-1 (STAT-1), phospho-ataxia telangiectasia and rad3-related kinase-1 (ATR-1), and phospho-Bad were all provided by Cell Signaling Technology (Beverly, MA). Horseradish peroxidase-conjugated goat antirabbit IgG, goat antimouse, and donkey antigoat IgG were purchased from Jackson ImmunoResearch Laboratories (West Grove, PA). Cyanine 3-conjugated donkey antigoat IgG was provided by Rockland (Gilbertville, PA). Reverse transcriptase and Taq DNA polymerase were purchased from Promega (Madison, WI).

2.2 Extraction of anthocyanins from the fruit of bog blueberry

The edible bog blueberry (*Vaccinium uliginosum* L., Korean name "Deol-Jugk") was collected from the Mountain Beag-Du (North Korea) on 10 August 2005. The fresh fruits (100 g) were juiced with 100 mL water and filtered with Whatman No. 2 filter paper. The filtrate (100 mL) was adsorbed on Diaion HP-20 resin column (700 × 30 mm^2 id) and washed with water (*ca.* 1500 mL) for washing of sugar or the impure components, followed by ethanol (*ca.* 500 mL) for the anthocyanin-rich fraction. The obtained anthocyanin fraction was lyophilized and stored at −20°C.

2.3 HPLC and MS analyses of ATH-BBe

Anthocyanin separation was conducted on an RP YMC ODS H-80 column (4.6 × 250 mm^2 id, S-4 μm; YMC, Kyoto, Japan) using a Finnigan Surveyor HPLC system (ThermoQuest, San Jose, CA) [24, 25]. The mobile phase was composed of water containing 0.1% formic acid (solvent A) and 100% ACN containing 0.1% formic acid (solvent B). For the elution, the following gradient was employed: initial, 10% solvent B; 23 min, 40% solvent B; 26 min, 100% solvent B; 29 min, 100% solvent B; 32 min, 10% solvent B. The flow rate was 600 μL/min and the injection volume 10 μL. Eluted substances were detected at 517 nm with a photodiode-array detector (PDA) between 200 and 600 nm with a bandwidth of 1.0 nm.

For the identification of the major anthocyanins, the column elute was split, and 0.2 mL/min was directed to a Finnigan LCQ Advantage IT mass spectrometer (ThermoQuest) equipped with an ESI interface after passing through the flow cell of the PDA detector. Analysis was detected using positive ion monitoring at a capillary temperature of 250°C, spray voltage of 5.5 kV, capillary voltage of 2.3 V, and tube lens offset of 48 V. Spectral data were recorded with N_2 as collision gas (sheath gas of 28 arbitrary units). The detection of each compounds were confirmed using *m*/*z* value following MS/MS of *m*/*z* value. The MS/MS collision energy was set to 35%. For purposes of presentation, data for figures in this paper were collected using dual analysis in full-scan mode from 100 to 1000 amu and MS/MS modes. Data were collected and processed using the Xcalibur 1.4 version software program (Thermo Electron, Waltham, MA).

The final concentrations of the prepared bog blueberry solutions for the HPLC analysis were 5 g/L. ATH-BBe was dissolved in DMSO for cell culture; its final culture concentration was ≤0.05%.

2.4 Culture and UV-B irradiation of fibroblasts

Human dermal fibroblasts were cultured in DMEM containing 10% FBS, 2 mmol/L glutamine, 100 000 U/L penicillin, and 100 mg/L streptomycin at 37°C humidified atmosphere of 5% CO_2 in air. The cells were plated at 90–95% confluence in all experiments. The UV-B light source (312 nm) was provided from Bio-Sun lamps (Vilber-Lourmat, Marine, France). Dermal fibroblasts were pretreated with 1–10 mg/L ATH-BBe, exposed to 100 mJ/cm^2 UV-B in PBS and further incubated for 48 h in DMEM. In our previous study [12], it was shown that the irradiation energy of UV-B at ≥100 mJ/cm^2 significantly and dose-dependently reduced the viability of 48 h-cultured cells in a range of 50–3000 mJ/cm^2. Accordingly, fibroblasts were exposed to UV-B at the irradiation energy of 100 mJ/cm^2.

After challenge of dermal fibroblasts with UV-B, MTT assay was performed to quantitatively determine cellular viability [26]. The cells were incubated in a fresh medium containing 1 g/L MTT for 3 h at 37°C. After removal of unconverted MTT, the purple formazan product was dissolved in 0.5 mL isopropanol. Absorbance of formazan dye was measured at λ = 570 nm. In addition, the cellular generation of ROS was measured by DCF fluorescence [26]. The cells were treated for 30 min at 37°C with 10 μmol/L DCHF-DA in prewarmed DMEM. The cell images were photographed by a fluorescence microscope.

2.5 Western blot analysis

Western blot analysis was carried out using whole cell lysates and culture media prepared from human dermal fibroblasts [27]. Whole cell lysates were prepared in a lysis buffer containing 1% β-mercaproethanol, 1 mol/L β-glycerophosphate, 0.1 mol/L Na_3VO_4, 0.5 mol/L NaF, and protease inhibitor cocktail. Cell lysates containing equal amounts of total proteins or equal volumes of culture supernatants were electrophoresed on 6–12% SDS-PAGE gels and transferred onto a nitrocellulose membrane. Nonspecific binding was blocked by soaking the membrane in a TBS-T buffer (50 mmol/L Tris-HCl (pH 7.5), 150 mmol/L NaCl, and 0.1% Tween 20) containing 3% BSA for 3 h. The membrane was incubated with monoclonal mouse antihuman MMP-1, polyclonal goat antibodies (human MMP-8, human MMP-13, human type1 collagen, and human type1 procollagen) and polyclonal rabbit antibodies (human NF-κB, human IκB, human phospho-IκB, human phospho-ASK1 (Ser 967), human phospho-JNK (Thr 183/Tyr 185), human phospho-p38 MAPK (Thr 180/Tyr 182), human phospho-c-Jun (Ser 73), human phospho-p53 (Ser 46). human phospho-p53 (Ser 15), human phospho-STAT1 (Ser 727), human phospho-ATR (Ser 428), and human phospho-Bad (Ser 112)). The membrane was then incubated with a secondary antibody, a goat antirabbit IgG, goat antimouse IgG, or donkey antigoat IgG conjugated to horseradish peroxidase. The protein levels were determined by using Supersignal West Pico Chemiluminescence detection reagents (Pierce Biotechnology, Rockford, IL), and Konica X-ray film (Konica, Tokyo, Japan). Incubation with polyclonal mouse antihuman β-actin antibody was performed for comparative control.

2.6 p53 nucleofection

This study attempted to determine the involvement of p53 signaling in UV-B-triggered bad activation. Human-specific p53 small interfering RNA (siRNA) kit (Cell Signaling Technology) was used to specifically inhibit p53 expression. Dermal fibroblasts were transfected with p53-targeted siRNA by electroporated with a NucleofectorTM (Amaxa, Koeln, Germany) according to the optimized protocols provided by the manufacturer recommendations. Briefly, cells were pelleted and gently resuspended in 100 μL of nucleofector, mixed with 2 μL of transfection reagent and 6 μL of 10 μmol/L human-specific p53 siRNA in an Amaxa cuvette, and pulsed in the nucleofector device (program U-23). Transfected cells were transferred into prewarmed fresh medium in six-well plates. After 24 h nucleofection, the transfected cells were exposed to 100 mJ/cm^2 UV-B prior to 18 h incubation and cell lysates were prepared for Western blot analysis.

2.7 Immunocytochemistry

After fibroblasts grown on 24-well glass slides were washed with PBS containing 0.05% Tween 20, cells were fixed with 4% ice-cold formaldehyde for 30 min and treated for 2 min with 0.1% Triton-X100 and 0.1% citric acid in PBS. For blocking any nonspecific binding, cells were incubated with 20% FBS for 1 h. After washing fixed cells, polyclonal goat antihuman antibody (type 1 procollagen or collagen) was sufficiently added and incubated overnight at 4°C. The cells were incubated with FITC conjugated antigoat IgG (1:10 000) for procollagen and cyanine 3-conjugated antigoat IgG (1:10 000) for collagen as a secondary antibody. Fluorescent images were obtained by a fluorescence microscopy with an Olympus BX51 fluorescent microscope with differential interference contrast and reflected light fluorescence.

2.8 Analyses of reverse transcriptase-polymerase chain reaction (RT-PCR) and real-time PCR

Following culture protocols, total RNA was isolated from human dermal fibroblasts using a commercially available Trizol reagent kit (Invitrogen, Carlsbad, CA). The RNA (2 μg) was reversibly transcribed with 200 units of reverse transcriptase and 0.5 g/L oligo-$(dT)_{15}$ primer (Bioneer, Korea).

2.8.1 RT-PCR

The expression of mRNA transcripts of MMP-1 (forward primer: 5′-ATTCTACTGATATCGGGGCTTTGA-3′, reverse primer: 5′-ATGTCCTTGGGGTATCCGTGTAG-3′), and β-actin (forward primer: 5′-GACTACCTCATGAAG ATC-3′, reverse primer: 5′-GATCCACATCTGCTGGAA-3′) were evaluated by RT-PCR as previously described [28]. The PCR was carried out in a buffer (10 mmol/L Tris-HCl (pH 9.0), 25 mmol/L $MgCl_2$, 10 mmol/L dNTP, 5 units of Taq DNA polymerase and 10 μmol/L of each primer) and terminated by heating at 94°C for 10 min. After thermocycling and electrophoresis of 25 μL PCR products on 2% agarose-formaldehyde gel, the bands were visualized using a TFX-20 M model-UV transilluminator (Vilber-Lourmat) and gel photographs were obtained. The absence of contaminants was routinely checked by the RT-PCR assay of negative control samples without a primer addition.

2.8.2 Real-time PCR

The levels of mRNA transcripts of procollagen type 1 (forward primer: 5′- TTCTTGCAGTGGTAGGTGATGTTC-3′, reverse primer: 5′- GCTACCCAACTTGCCTTCATG-3′), MMP-1 (forward primer: 5′-ACGGATACCCCAAGGA-CATCT-3′, reverse primer: 5′- CTCAGAAAGAGCAG-CATCGATATG-3′), and glyceraldehyde-3-phosphate dehydrogenase (GAPDH) (forward primer: 5′- GAAGGT-GAAGGTCGGAGTC-3′, reverse primer: 5′- GAA-GATGGTGATGGGATTTC-3′) were quantified by real-time RT-PCR using SYBR Green PCR kit (Quagen, Valencia, CA) and data analysis of real-time RT-PCR results and calculation of the relative quantitations was performed using the Delta CT analysis by the Rotor-gene software version 6.0 (Corbett Research, Australia). The housekeeping gene GAPDH was used for internal normalization. The standard PCR conditions were 95°C for 10 min, then 40 cycles at 95°C (10 s), 60°C (15 s), and 72°C (20 s), followed by the melting curve analysis.

2.9 ELISA

The cytokine secretion from fibroblasts UV-B-irradiated was determined using ELISA. Collected culture media were assayed for secretion of TNF-α, interleukin (IL)-8, IL-6, and IL-1β using ELISA kits (R&D Systems, Minneapolis, MN) according to the manufacturer's instructions.

2.10 Nuclear extract preparation

Cytosolic and nuclear protein fractions were prepared by a detergent lysis procedure to determine the translocation of NF-κB [28]. The cells were lysed in 10 mmol/L HEPES buffer (pH 7.9, 10 mmol/L KCl, 0.4 mmol/L PMSF, 1 mmol/L DTT, 1 mmol/L EDTA, 0.5% Nonidet P40, 20 mg/L of each of aprotinin, antipain, and leupeptin) and incubated on ice for 1 h. Nuclei were pelleted by a centrifugation at 3000 × *g* for 20 min. Proteins were extracted from nuclear pellets by incubation in a high-salt buffer containing 420 mmol/L NaCl, 20 mmol/L HEPES ((pH 7.9), 0.4 mmol/L PMSF, 1 mmol/L DTT, 1 mmol/L EDTA, 20% glycerol, and 10 mg/L of each of aprotinin, antipain, and leupeptin) at 4°C with vigorous shaking. The nuclear debris was pelleted by a brief centrifugation at 20 000 × *g* for 30 min and the supernatant was stored for further experiments.

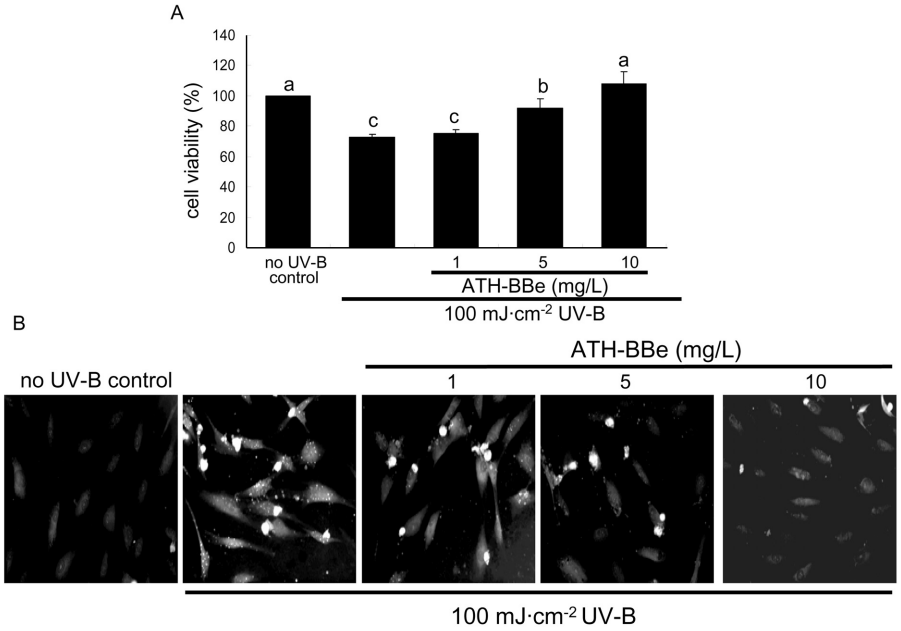

Figure 1. Cell viability (A) and intracellular oxidant generation (B) in ATH-BBe-treated human dermal fibroblasts challenged with UV-B irradiation. Confluent fibroblasts were left untreated or stimulated with 100 mJ/cm^2 UV-B prior to incubation for 48 h with ATH-BBe. Cell viability was measured using MTT assay and presented as means ± SEM from three independent experiments with multiple estimations (A). Values not sharing a letter are different at $p < 0.05$. Confluent cells were left untreated or stimulated by 100 mJ/cm^2 UV-B prior to incubation for 48 h and loaded with DCHF-DA. Oxidant generation was measured by DCF fluorescence (B). Representative fluorescent images of no UV-B controls and UV-B-irradiated cells were measured using a fluorescence microscopy. Magnification: 200-fold.

2.11 Data analysis

The results are presented as means ± SEM for each treatment group. Statistical analyses were conducted using Statistical Analysis Systems (SAS Institute, Cary, NC). Significance was determined by one-way ANOVA followed by Duncan range test for multiple comparisons and were considered significant at $p < 0.05$.

3 Results

3.1 Identification of anthocyanins rich in bog blueberry

The UV/Vis and ESI-MS/MS spectral data showed various anthocyanins quantified at 517 nm; five anthocyanins were detected in bog blueberry fruit juice and identified as cyanidin-3-glucoside, petunidin-3-glucoside, malvidin-3-glucoside, and delphinidin3-glucoside, and delphinidin-3-arabinoside (Table 1). The MS/MS spectra of anthocyanins provided clear and characteristic fragmentation pattern data. Masses for the aglycones are (MW): cyanidin, 287; petunidin, 317; malvidin, 331; delphinidin, 303.

3.2 Inhibition of UV-B-triggered toxicity of fibroblasts by ATH-BBe

To examine cell viability in UV-B-exposed human dermal fibroblasts, MTT analysis was conducted. The UV-B irradiation reduced the viability with >30% cell killing at 100 mJ/cm^2 (Fig. 1A). When ATH-BBe was added to UV-B-irradiated cells in concentrations between 1 and 10 mg/L, the viability was dose-dependently increased. The UV-B induction of ROS was dampened by adding ATH-BBe at doses of ≥5 mg/L, evidenced by a disappearance of DCF staining (Fig. 1B). ROS generation enhanced by UV-B was most likely responsible for dermal fibroblast toxicity. Thus, ATH-BBe appears to be capable of inhibiting an accumulation of intracellular ROS in fibroblasts damaged by oxidative stress cause by UV-B.

UV-B light-triggered oxidative stress appeared to elicit DNA damage leading to rapid activation of ATR-1 and induce subsequent phosphorylation of the transcription factor p53 at Ser15 (Figs. 2A and B). Pretreatment of UV-B-exposed fibroblasts with 10 mg/L ATH-BBe abolished activation of ATR and p53. It was deemed that the p53 activation was upregulated by ATR-1 activation in

Table 1. Identification of major anthocyanins detected in the fruit of bog blueberry[a)]

Compounds	R_t (min)	UV/Visλ max (nm)	LC – ESI – MS		Structure
			m/z $[M + H]^+$	MS/MS fragments[b)]	
1	9.21	233, 280, 517	449	448.76 (Cy + Glc)	Cyanidin-3-glucoside
–	–	–	–	286.99 $(Cy)^+$	–
2	9.81	233, 278, 521	479	478.74 (Pt + Glc)	Petunidin-3-glucoside
–	–	–	–	316.96 $(Pg)^+$	–
3	10.70	234, 278, 525	493	492.82 (Mv + Glc)	Malvidin-3-glucoside
–	–	–	–	330.95 $(Mv)^+$	–
4	17.12	253, 356	465	464.67 (Dp + Glc)	Delphinidin-3-glucoside
–	–	–	–	302.98 $(Dp)^+$	–
5	18.69	255, 356	435	434.66 (Dp + Ara)	Delphinidin-3-arabinoside
–	–	–	–	302.97 $(Dp)^+$	–

a) Peaks 1 – 5 were identified based on photo didode array (PDA) absorbance and mass fragmentation pattern.
b) Fragments: cyanidin (Cy); glucoside (Glc); petunidin (Pt); malvidin (Mv); delphinidin (Dp); arabinoside (Ara).

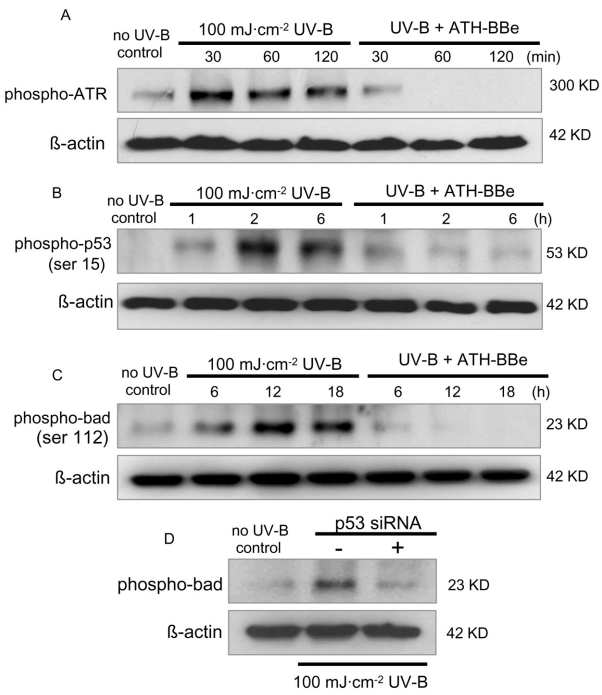

Figure 2. Western blot data showing phosphorylation of ATR (A), p53 at Ser15 (B) and Bad (C) in UV-B-exposed and ATH-BBe-treated human dermal fibroblasts. Confluent fibroblasts were exposed to 100 mJ/cm^2 UV-B incubation in the presence of 10 mg/L ATH-BBe. Phosphorylation of Bad by UV-B was examined in human dermal fibroblasts transfected by p53 siRNA (D). Total cell protein extracts were electrophoresed, followed by Western blot analysis with a primary antibody against each protein (three independent experiments). β-Actin protein was used as an internal control.

response to UV-B-elicited DNA damage. In addition, the UV-B-elevated phosphorylation of proapoptotic Bad gene protein was blocked by an addition of ATH-BBe (Fig. 2C). Furthermore, the siRNA-mediated knockdown of p53 expression augmented UV-B-dependent expression of phosphorylated Bad in dermal fibroblasts (Fig. 2D), indicating that the phosphorylation of p53 at Ser15 led to fibroblast apoptosis.

3.3 Inhibitory effects of ATH-BBe on fibroblast collagen collapse of UV-B irradiation

Western blot data revealed that UV-B exposure caused a marked reduction in the expression level of procollagen (Fig. 3A). The diminished procollagen levels were dose-dependently boosted by adding ATH-BBe to fibroblasts. Consistent with the blot data, the immunocytochemical staining with a specific procollagen antibody confirmed that ATH-BBe reversed the UV-B-induced reduction in the procollagen levels; the favorable effects were evident with ≥5 mg/L ATH-BBe. UV-B light at 100 mJ/cm^2 markedly attenuated intracellular collagen levels, indicative of enhanced collagen degradation (Fig. 3B). When ATH-BBe at doses of 1 – 10 mg/L was added to dermal fibroblasts exposed to UV-B, the cellular level of collagen protein was restored in a dose-dependent manner. Additionally, the collagen secretion was dampened in UV-B-exposed fibroblasts, whereas pretreatment with ATH-BBe boosted collagen levels in culture media (Fig. 3C). The real time PCR data showed that UV-B diminished the mRNA levels of procollagen, suggesting the downregulation of procollagen protein at transcriptional levels (Fig. 3D). In contrast, 10 mg/L ATH-BBe-treated and UV-B-irradiated cells elevated procollagen mRNA levels.

3.4 Inhibition of collagenolytic MMP secretion by ATH-BBe

Collagen is synthesized in a precursor form of procollagen and secreted out of dermal cells. It was explored whether production of collagenolytic MMP was responsible for UV-B light-promoted collagen degradation and whether ATH-

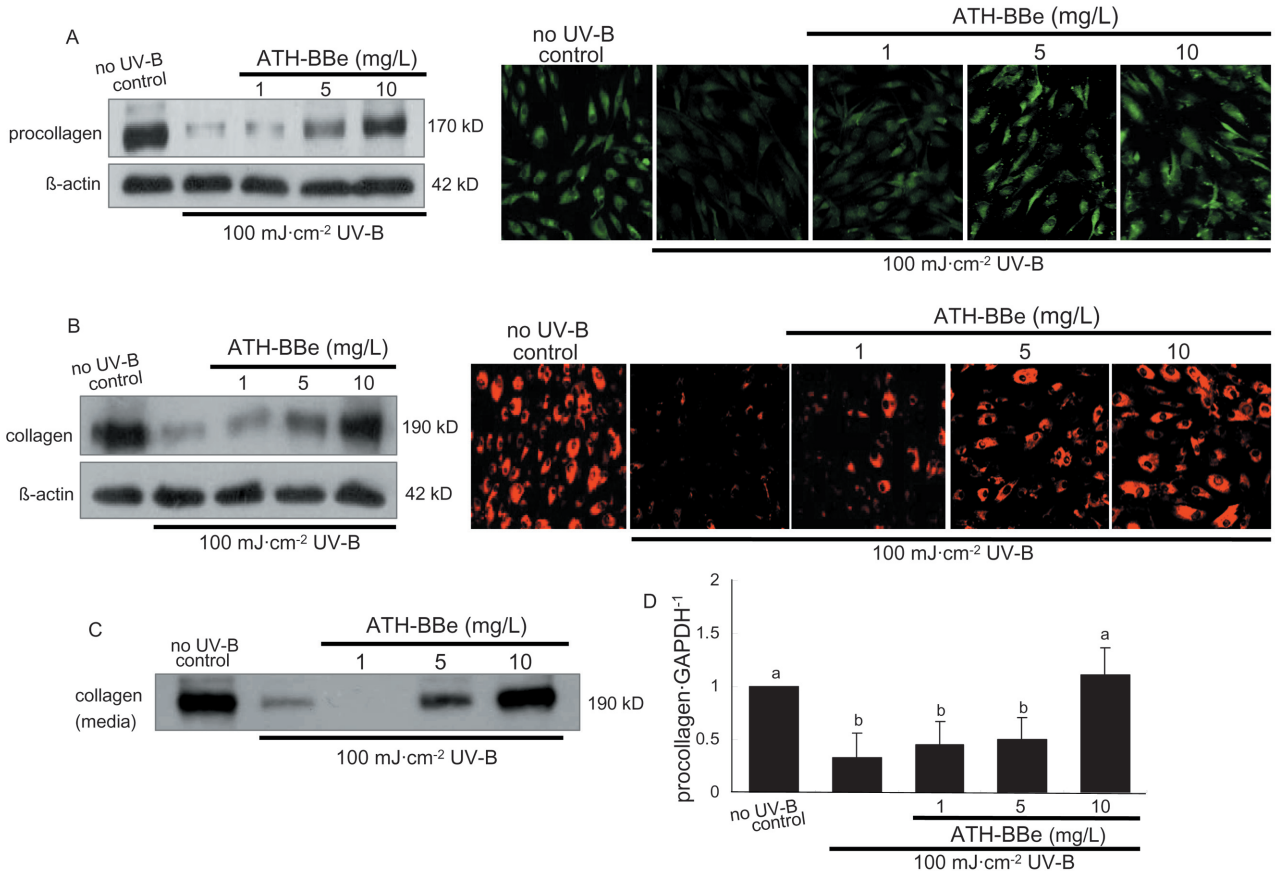

Figure 3. Inhibitory dose responses of ATH-BBe to levels of type 1 procollagen (A) and collagen (B) in 100 mJ/cm^2 UV-B-irradiated human dermal fibroblasts. Cell lysates were subjected to 6% SDS-PAGE and Western blot analysis with a primary antibody against type 1 procollagen and collagen. β-Actin protein was used as an internal control. In immunocytochemical experiments, cells were fixed and then incubated with goat antihuman type 1 procollagen (A) and collagen (B). Antibody localization was detected with FITC conjugated donkey antigoat IgG (A) or Cyanine 3-conjugated donkey antigoat IgG (B) using a fluorescence microscopy. Magnification: 100-fold (A). Secretion of collagen (C) in culture media was measured using Western blot analysis and transcriptional levels of procollagen mRNA (D) examined using real-time RT-PCR in ATH-BBe-treated and UV-B-irradiated human dermal fibroblasts. GAPDH gene was used as an internal control for the coamplification with procollagen. The bar graphs (means ± SEM, $n = 3$) represent quantitative mRNA transcript levels of procollagen relative to GAPDH. Values not sharing a letter refer to significant different at $p < 0.05$.

BBe was capable of suppressing MMP secretion in UV-B-irradiated fibroblasts. The UV-B irradiation markedly increased secretion of MMP-1, MMP-8, and MMP-13, whereas the treatment of irradiated cells with 1 – 10 mg/L ATH-BBe downregulated the production of all of three enzymes in similar dose dependent ways (Fig. 4A). Elevated MMP production was reversed by a treatment with ≥5 mg/L ATH-BBe.

There were moderate signals for the basal mRNA expression of MMP-1 in quiescent fibroblasts (Fig. 4B). In contrast, the expression of MMP-1 mRNA was increased in 24 h-UV-B-stimulated dermal fibroblasts. However, the RT-PCR data showed that the UV-induced mRNA accumulation level of MMP-1 was diminished in cells treated with 10 mg/L ATH-BBe. Furthermore, the MMP-1 gene expression was confirmed by quantitative real time-PCR (Fig. 4C). UV-B sharply induced MMP-1 transcript expression by ≈five-fold compared to that of no-UV-B control cells. The mRNA expression level of MMP-1 in cells treated with 10 mg/L ATH-BBe was dropped off. Indeed, this was consistent with a substantial attenuation of MMP-1 production due to ATH-BBe addition shown in Fig. 4A. These results imply that ATH-BBe inhibits the secretion of MMP proteins *via* a direct modulation at their gene transcriptional levels.

3.5 Abolishment of release of inflammatory cytokines by ATH-BBe

The UV-B irradiation promoted the 48 h-production of the proinflammatory cytokines of IL-1β, IL-6, IL-8, and TNF-α with different magnitudes, as quantified by ELISA

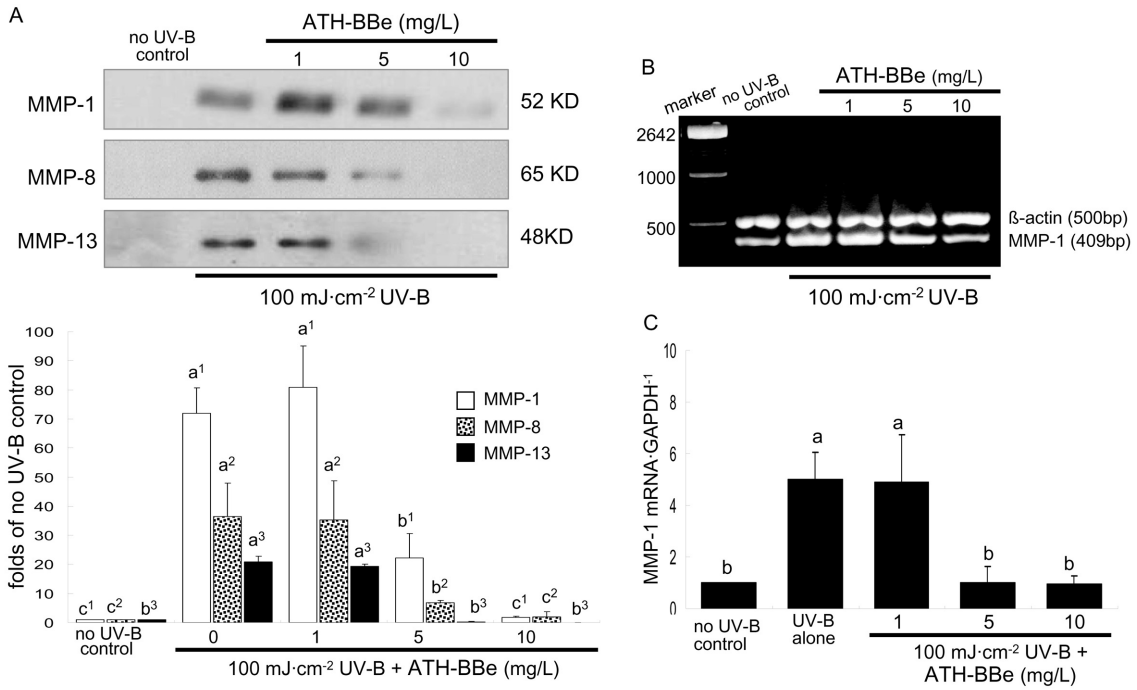

Figure 4. Inhibitory dose responses of ATH-BBe to induction of respective protein (A) and mRNA (B and C) of MMP-1, MMP-8, and MMP-13 in UV-B irradiated human dermal fibroblasts. After cells were exposed to 100 mJ/cm^2 UV-B and pretreated with 1 – 10 mg/L ATH-BBe for 48 h, conditioned culture media were collected and subjected to 10% SDS-PAGE, followed by Western blot analysis with respective primary antibody of MMP-1, MMP-8, and MMP-13 (A). Bands are representative of three independent experiments and the bar graphs (bottom panel of A, means ± SEM) represent secretion levels of MMP proteins. Values not sharing a letter (+superscripts) refer to significant different at $p < 0.05$. The RT-PCR data (B) and real time-PCR (C) showing transcriptional levels of MMP-1 mRNA in ATH-BBe-treated and UV-B-exposed human dermal fibroblasts. β-Actin and GAPDH genes were used as an internal control for the coamplification with MMP-1. The bar graphs (panel C, means ± SEM, $n = 3$) represent quantitative mRNA transcript levels of MMP-1 relative to GAPDH. Values not sharing a letter refer to significant different at $p < 0.05$.

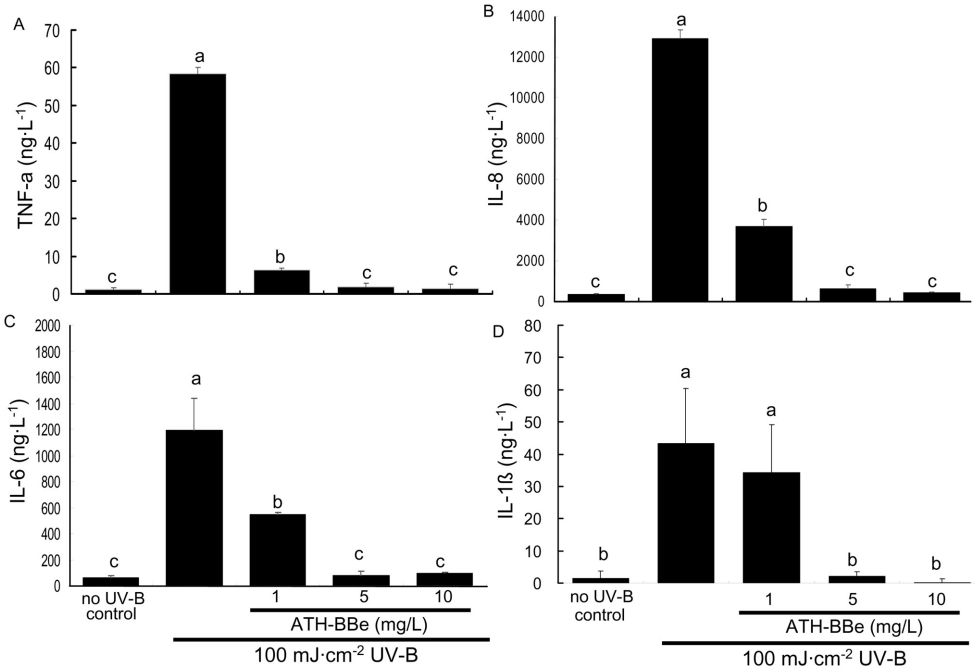

Figure 5. Prevention of TNF-α, IL-8, IL-6, and IL-1β secretion by ATH-BBe in UV-B-exposed human dermal fibroblasts. Confluent fibroblasts were untreated or stimulated with 100 mJ/cm^2 UV-B prior to incubation for 48 h with ATH-BBe. The cell culture medium were collected and measured using ELISA. Data represent means ± SEM from three independent experiments with multiple estimations. Values not sharing a letter are different at $p < 0.05$.

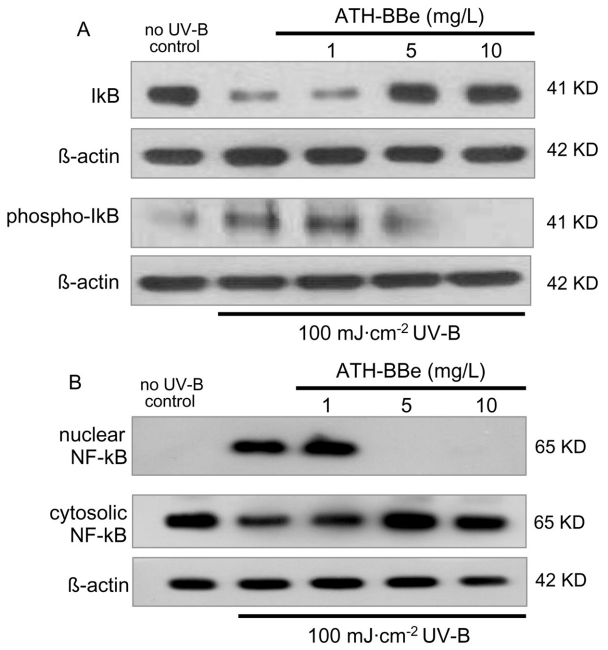

Figure 6. Inhibition of IκBα degradation from NF-κB complex (A) and translocation of NF-κB p65 (A) by ATH-BBe in 100 mJ/cm^2 UV-B-irradiated human dermal fibroblasts. Samples (whole cell lysate for IκB, cytosolic and nuclear protein fractions for NF-κB) of cells pretreated with 1 – 10 mg/L ATH-BBe and irradiated to 100 mJ/cm^2 UV-B were electrophoresed on 8% SDS-PAGE gel, followed by Western blot analysis with a primary antibody against each protein (three independent experiments). β-Actin protein was used as an internal control.

(Fig. 5). The UV-B potency for elevating secretion of these cytokines were in the order of IL-8 > IL-6 ≫ TNF-α ≥ IL-1β; IL-8 was secreted as much as >10 mg/L in response to UV-B exposure. The inhibitory effects of ATH-BBe on individual secretion of these cytokines in UV-B-exposed dermal fibroblasts were achieved with similar patterns (Fig. 5).

3.6 ATH-BBe blockade of NF-κB activation and MAPK signaling

Immunoblot analysis revealed that UV-B light triggered phosphorylation of IκB in human dermal fibroblasts, indicative of increase in IκB dissociation from NF-κB complex (Fig. 6A). In contrast, pretreatment with ATH-BBe reduced phosphorylation of IκB in UV-B-irradiated fibroblasts in a dose-dependent way. Additionally, the nuclear translocation of NF-κB was further examined in UV-B-irradiated fibroblasts. An increase of NF-κB p65 in the nucleus was observed following an exposure of cells to 100 mJ/cm^2 UV-B, indicating that UV-B enhanced nuclear translocation of NF-κB (Fig. 6B). UV-B-irradiated cells treated with ≥5 mg/L ATH-BBe diminished nuclear NF-κB levels with enhancing levels of cytosolic NF-κB. Thus, microgram doses of ≥5 mg/L were required for achieving full inhibitory effect of ATH-BBe on NF-κB translocation and transcriptional activity in dermal fibroblast photoaging models.

This study attempted to determine whether ATH-BBe may alleviate photoaging in UV-B-irradiated fibroblasts through interfering with ASK-1-MAPK signaling cascades. The UV-B-irradiated fibroblasts rapidly induced phosphorylation of JNK and p38 MAPK pertaining to ASK-1 (Fig. 7A). In addition, it was also observed that ATH-BBe inhibited activation of nuclear transcription factors of the JNK downstream target of c-Jun, and of the p38 MAPK downstream targets of p53 at Ser 46 and STAT-1 (Fig. 7B). There were multiple pathways of p53 phosphorylation upon exposure to UV-B light (Fig. 2B). When 10 mg/L ATH-BBe was treated with fibroblasts exposed to UV-B, the ASK-1-diverged JNK, and p38 MAPK signaling pathways were markedly attenuated (Fig. 7). Accordingly, ATH-BBe blocked the regulation of ASK-1-MAPK signal transduction and related pathways leading to transcription of gene proteins involved in collagen degradation and inflammation as well as apoptosis.

4 Discussion

The current study elucidated the action mechanisms of ATH-BBe in UV-B irradiation-induced collagen degradation and inflammatory mediator production in human dermal fibroblasts. UV-B is one of the most important external stimuli that affect skin by inducing cancer, premature skin aging, inflammation, and cell death [4 – 6, 12]. Six major observations were obtained from this study. (i) Five anthocyanins were detected in bog blueberry fruit juice and identified as cyanidin-3-glucoside, petunidin-3-glucoside, malvidin-3-glucoside, and delphinidin3-glucoside, and delphinidin-3-arabinoside. (ii) ATH-BBe at doses of 1 – 10 mg/L mitigated the UV-B irradiation-induced human dermal fibroblast toxicity with blockade of ROS production leading to apoptotic Bad activation. (iii) ATH-BBe reversed procollagen expression downregulated in UV-B-exposed fibroblasts at transcriptional levels. (iv) UV-B augmented secretion of collagenolytic enzymes of MMP-1, MMP-8, and MMP-13, thereby enhancing collagen degradation, which was diminished in ATH-BBe-treated fibroblasts. (v) ATH-BBe dampened production of inflammatory cytokines responsible for UV-B-elicited photoaging responses. (vi) ATH-BBe attenuated UV-B-triggered dermal collagen destruction through hampering nuclear activation of NF-κB and signaling pathways of JNK and p38 MAPK. These overall results demonstrate that ATH-BBe has the capability to prevent UV-B-induced skin photoaging at its pharmaco-nutraceutical doses. The capability of edible ATH-BBe to block the UV-B-induced collagen destruction and inflammatory responses was possibly mediated *via* transcriptional mechanisms of NF-κB and MAPK signaling.

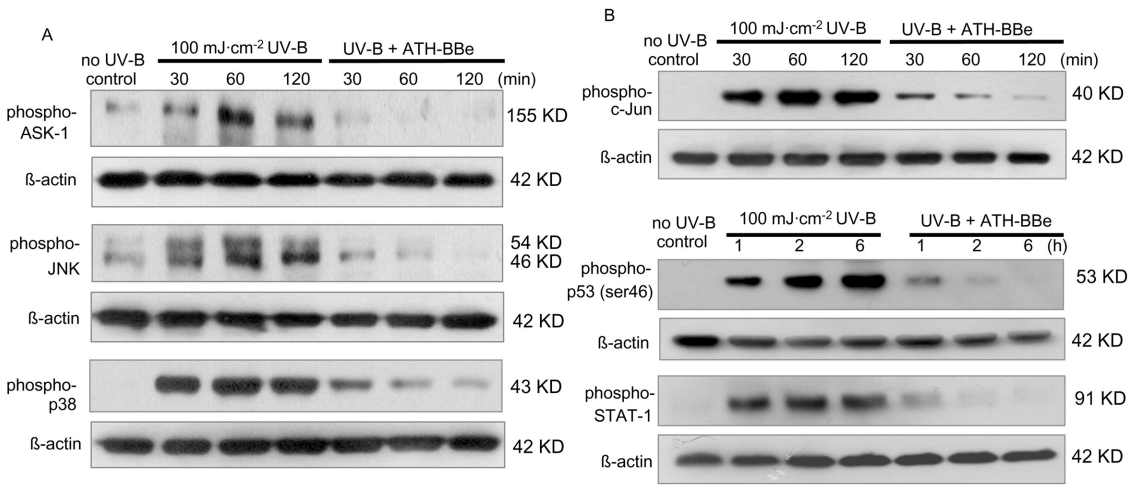

Figure 7. Inhibitory effects of ATH-BBe on phosphorylation (A) of ASK, JNK, p38 MAPK, and activation of transcription factors (B) of c-Jun, p53 (ser 46) and STAT-1 in UV-B-exposed human dermal fibroblasts. Confluent fibroblasts were exposed to 100 mJ/cm^2 UV-B incubation in the presence of 10 mg/L ATH-BBe. Total cell protein extracts were electrophoresed, followed by Western blot analysis with a primary antibody against each protein (three independent experiments). β-Actin protein was used as an internal control.

Prolonged or repeated sun exposure is known to elicit cutaneous damages such as sunburn or long-term effects such as photoaging and UV-induced skin cancer. These damages are clearly linked to the biological effects of solar UV light including radiation of UV-B (290 – 320 nm) and UV-A (320 – 400 nm) on the epidermis and dermis [29]. Although the amount of UV-B is far less than UV-A, it is mostly responsible for photocarcinogenesis [5]. When the UV-B energy source of 100 mJ/cm^2 were irradiated on cultured fibroblasts for 48 h, cell viability was diminished up to >30%. The solar UV irradiation promotes the formation of free radicals that directly damage DNA by inducing lesions and pyrimidine photoproducts [5]. It was assumed that the UV-B-induced fibroblast toxicity in this study was in consequence of ROS formation. The DCF staining showed that 100 mJ/cm^2 UV-B resulted in oxidative stress by accompanying excessive generation of ROS. Thus, the strategies to prevent early pathological events induced by UV light may be useful for providing efficient and adequate photoprotection. One approach to ameliorate adverse effects of UV-B on the skin is the use of antioxidants scavenging and quenching ROS [30]. Use of botanical antioxidants appears to be an effective strategy for reducing incidences of UV-mediated oxidative photodamage [16]. Several studies have shown that polyphenols possessing antioxidant properties are promise agents reducing the risk of skin diseases [12, 17 – 20]. EGCG protected against the oxidative cellular and genotoxic damage of UV-A radiation [17].

It has been reported that UV-B-triggered ROS induces MMP in photoaged skin, which affects connective tissue breakdown [9]. In addition, UV irradiation hampered ECM preservation in premature skin aging [31]. Approaches to avert photodamage resulted from biological events initiated by UV include inhibition of MMP activity to prevent ECM damage. Antioxidant EGCG prevented collagen collapse through inhibiting MMP activity UV-B-irradiated human dermal fibroblasts [12]. The UV-B exposure to cultured dermal fibroblasts elicited dramatic reduction of collagen with a marked increase in the MMP secretion, which was reversed by ATH-BBe. Oral administration of green tea polyphenols resulted in inhibition of UV-B-induced expression of ECM degrading MMP including MMP-2, MMP-3, MMP-7, and MMP-9 in hairless mouse skin [32], suggesting that green tea polyphenols as a dietary supplement could be useful to attenuate solar UV-B light-induced skin carcinogenesis [33]. Therefore, dietary interventions with plant extracts containing anthocyanins have beneficial effects toward diverse skin degenerative diseases initiated by solar UV radiation.

Inflammation and the resulting free radical generation play an important role in the intrinsic and photoaging of human skin *in vivo* [34]. UV irradiation causes increased synthesis and release of proinflammatory mediators from a variety of skin cells leading to infiltration and activation of neutrophils and other phagocytic cells into the skin [7]. Thus, inflammatory mechanisms may accentuate the effect of UV radiation to amplify direct damaging effects on molecules and cells which cause photoaging. It was shown that inflammation activates various MMP leading to abnormal ECM degradation and accumulation of nonfunctional matrix components in the dermal and epidermal compartments, contributing to the etiology of photoaging [7]. The present study showed that the UV-B exposure induced various proinflammatory cytokines possibly linked to the transcription of MMP resulting in the fibroblast collagen collapse. Inhibition of the cutaneous inflammatory response to

photoskin interactions is crucial to comprehensively protect the skin from adverse solar effects. Prevention of inflammation using anti-inflammatory compounds, *e.g.*, cyclooxygenase inhibitors and inhibitors of cytokine generation, is one of strategies to prevent photoaging triggered by UV [7, 13]. It was observed that ATH-BBe dampened fibroblast secretion of proinflammatory cytokines augmented by UV-B. Red orange extract was potentially able to efficiently counteract UV-B-induced responses pertaining to cellular oxidative stress-related inflammation and apoptosis in human keratinocytes [34]. Treatment of silymarin, a flavonoid from milk thistle, inhibited UV-induced oxidative stress generated by both epidermal and dermal cells through targeting infiltrating CD11b + macrophages in the skin [19].

Previous studies have shown that antioxidants inhibit UV-induced oxidative stress in the skin, proposing as promise agents reducing the risk of skin diseases [10 – 12, 15]. However, the cellular targets responsible for the inhibition of UV-induced oxidative stress and inflammation leading to photoaging by antioxidants are not clearly defined. UV-B-light-initiated skin aging and nonmelanoma skin cancer may be averted by targeting cellular signaling [35]. Damage of dermal cells induced by UV light at the molecular levels elicits the activation of transcription factor pathways, which in turn modulate the expression of diverse UV-responsive genes [5, 35]. The present study revealed that UV-B irradiation enhanced the activation of apoptotic Bad protein of dermal fibroblasts through triggering p53 signaling by ATR activated due to DNA damage. In addition, ATH-BBe appeared to inhibit the apoptotic toxicity of fibroblasts by hampering the ATR-p53-Bad signaling cascade. Delphinidin, an anthocyanidin in pigmented fruits and vegetables, protected keratinocytes and mouse skin against UV-B mediated oxidative stress and cellular apoptosis *via* reducing DNA damage and boosting Bcl-2 family [30]. Naringenin, a naturally occurring citrus flavonone, exhibited an antiapoptotic effect in p53-mutant human HaCaT keratinocytes by enhancing the removal of UV-B-induced cyclobutane pyrimidine dimers in genomic DNA and by modulating UV-B-induced caspase cascade pathway [36]. Additionally, a soybean isoflavone genistein substantially inhibited UV light-induced skin carcinogenesis, photodamage, and cutaneous aging through preventing DNA damage and downregulating activated signal transduction cascades [37]. This study provides a molecular basis for the action of anthocyanins as a promising natural flavonoid in preventing skin aging and carcinogenesis.

Oxidative stress in photocarcinogenesis may cause activation of transcription factors including NF-κB and AP-1 [35]. These transcription factor pathways and the crosstalk between them in response to UV-B exposure may help with the development of new dietary strategies for the prevention of UV-B-induced skin aging. ATH-BBe attenuated release of proinflammatory cytokines, which appeared to be mediated through hindering NF-κB activation and other transcriptional factors. In a recent study [38], cyanidin-3-rutinoside, an anthocyanin found in abundance in black raspberries was found to contribute to the inhibition of UV-B-induced signaling pathways leading to activation of NF-κB in mouse epidermal cells. Dietary grape seed proanthocyanidins inhibited UV-B-induced activation of NF-κB/p65 to target genes pivotal in inflammation and cellular proliferation, whereby the expression of cyclin D1, inducible nitric oxide synthase, and cyclooxygenase-2 was dampened in the skin [22].

This study hypothesized that ATH-BBe blocks MMP-mediated photoaging by influencing the UV-B-modulated MAPK-dependent pathways. It has been reported that oxidative stress in UV light-induced skin carcinogenesis may cause activation of transcription factors and protooncogenes such as c-fos and c-Jun as well as genetic instability [5]. In addition, the molecular mechanisms by which UV light causes photoaging involve activation of downstream signal transduction through activation of MAPK pathways of JNK and p38 [12], and these signaling pathways activate nuclear AP-1 leading to an induction of collagenases that degrade skin connective tissue [11]. It is deemed that the ability of antioxidants to protect the skin from the adverse effects of UV-B radiation may be mediated *via* modulation of the MAPK signaling pathways. The current study revealed that ROS-quenching ATH-BBe retarded activation of JNK and p38 MAPK pathways linked to ASK-1 signaling which in turn converged in the nucleus of fibroblasts to activate c-Jun, STAT-1 and p53. Our data suggest that botanical compounds with antioxidative activities are able to protect against the adverse effects of UV radiation *via* modulations in MAPK signaling cascades in *in vitro* dermal cell and *in vivo* animal model systems. Genistein may prevent photoaging with inhibiting UV induction of both extracellular signal-regulated kinase (ERK1/2) and JNK activities [11]. Dietary polyphenols were found to have photoprotective effects in *in vivo* animal models through inhibition of UV-B-induced phosphorylation of MAPK protein family of JNK, p38 MAPK, and ERK1/2 [22, 39]. Additionally, silymarin pretreatment reversed the effect of UV irradiation on phosphorylation of Akt and activation of its downstream p53, followed by modulation of apoptotic and antiapoptotic gene proteins including Bax, Bcl-2, and Bcl-xL proteins leading to apoptosis in UV-irradiated human malignant melanoma cells [40].

In summary, the present results revealed the photoprotective actions of ATH-BBe on fibroblast collagen collapse and inflammatory responses pertaining to photoaging. ATH-BBe at pharmaco-nutraceutical doses mitigated UV-B-induced oxidant injury leading to DNA damage and subsequent activation of ATR-p53-Bad apoptotic pathway, which appeared to be responsible for the fibroblast survival. The contributions of NF-κB and MAPK signalings may entail photodamage caused by the destructing cascade of collagen initiated by UV. Therefore, dietary interventions

with botanical antioxidants such as edible ATH-BBe provide a promising rationale for the design and development of treatment strategies aimed at limiting sun light-induced cellular oxidative damage eliciting photoaging and skin cancer.

This study was supported by grants (KRF-2006-521-F00072 and Brain Korea 21) from Korea Research Foundation, grant (R01-2006-000-10896-0) from Korea Science & Engineering Foundation, and a grant (TG-06-1-003) from Ministry of Commerce, Industry and Energy, Korea.

The authors have declared no conflict of interest.

5 References

[1] Rogers, G. S., Gilchrest, B. A., The senile epidermis: Environmental influences on skin aging and cutaneous carcinogenesis, *Br. J. Dermatol.* 1990, *122*, 55 – 60.

[2] Goihman-Yahr, M., Skin aging and photoaging: An outlook, *Clin. Dermatol.* 1996, *14*, 153 – 160.

[3] Young, A. R., Cumulative effects of ultraviolet radiation on the skin: Cancer and photoaging, *Semin. Dermatol.* 1990, *9*, 25 – 31.

[4] Scharffetter-Kochanek, K., Brenneisen, P., Wenk, J., Herrmann, G., *et al*., Photoaging of the skin from phenotype to mechanisms, *Exp. Gerontol.* 2000, *35*, 307 – 316.

[5] Nishigori, C., Cellular aspects of photocarcinogenesis, *Photochem. Photobiol. Sci.* 2006, *5*, 208 – 214.

[6] Kennedy, M., Kim, K. H., Harten, B., Brown, J., *et al*., Ultraviolet irradiation induces the production of multiple cytokines by human corneal cells, *Invest. Ophthalmol. Vis. Sci.* 1997, *38*, 2483 – 2491.

[7] Pillai, S., Oresajo, C., Hayward, J., Ultraviolet radiation and skin aging: Roles of reactive oxygen species, inflammation and protease activation, and strategies for prevention of inflammation-induced matrix degradation – a review, *Int. J. Cosmet. Sci.* 2005, *27*, 17 – 34.

[8] Uitto, J., The role of elastin and collagen in cutaneous aging: Intrinsic aging versus photoexposure, *J. Drugs Dermatol.* 2008, *7*, s12 – s16.

[9] Brenneisen, P., Sies, H., Scharffetter-Kochanek, K., Ultraviolet-B irradiation and matrix metalloproteinases: From induction via signaling to initial events, *Ann. NY Acad. Sci.* 2002, *973*, 31 – 43.

[10] Sander, C. S., Chang, H., Hamm, F., Elsner, P., Thiele, J. J., Role of oxidative stress and the antioxidant network in cutaneous carcinogenesis, *Int. J. Dermatol.* 2004, *43*, 326 – 335.

[11] Kang, S., Chung, J. H., Lee, J. H., Fisher, G. J., *et al*., Topical N-acetyl cysteine and genistein prevent ultraviolet-light-induced signaling that leads to photoaging in human skin in vivo, *J. Invest. Dermatol.* 2003, *120*, 835 – 841.

[12] Bae, J. Y., Choi, J. S., Choi, Y. J., Shin, S. Y., *et al*., (–)Epigallocatechin gallate hampers collagen destruction and collagenase activation in ultraviolet-B-irradiated human dermal fibroblasts: Involvement of mitogen-activated protein kinase, *Food Chem. Toxicol.* 2008, *46*, 1298 – 1307.

[13] Zhan, H., Zheng, H., The role of topical cyclo-oxygenase-2 inhibitors in skin cancer: Treatment and prevention, *Am. J. Clin. Dermatol.* 2007, *8*, 195 – 200.

[14] Fineschi, S., Cozzi, F., Burger, D., Dayer, J. M., *et al*., Anti-fibroblast antibodies detected by cell-based ELISA in systemic sclerosis enhance the collagenolytic activity and matrix metalloproteinase-1 production in dermal fibroblasts, *Rheumatology* 2007, *46*, 1779 – 1785.

[15] Offord, E. A., Gautier, J. C., Avanti, O., Scaletta, C., *et al*., Photo-protective potential of lycopene, β-carotene, vitamin E, vitamin C and carnosic acid in UVA-irradiated human skin fibroblasts, *Free Radic. Biol. Med.* 2002, *32*, 1293 – 1303.

[16] Hsu, S., Green tea and the skin, *J. Am. Acad. Dermatol.* 2005, *52*, 1049 – 1059.

[17] Tobi, S. E., Gilbert, M., Paul, N., McMillan, T. J., The green tea polyphenol, epigallocatechin-3-gallate, protects against the oxidative cellular and genotoxic damage of UVA radiation, *Int. J. Cancer* 2002, *102*, 439 – 444.

[18] Meeran, S. M., Mantena, S. K., Elmets, C. A., Katiyar, S. K., (–)-Epigallocatechin-3-gallate prevents photocarcinogenesis in mice through interleukin-12-dependent DNA repair, *Cancer Res.* 2006, *66*, 5512 – 5520.

[19] Katiyar, S. K., Meleth, S., Sharma, S. D., Silymarin, a flavonoid from milk thistle (Silybum marianum L.), inhibits UV-induced oxidative stress through targeting infiltrating CD11b + cells in mouse skin, *Photochem. Photobiol.* 2008, *84*, 266 – 271.

[20] Lee, K. W., Kundu, J. K., Kim, S. O., Chun, K. S., *et al*., Cocoa polyphenols inhibit phorbol ester-induced superoxide anion formation in cultured HL-60 cells and expression of cyclooxygenase-2 and activation of NF-κB and MAPKs in mouse skin in vivo, *J. Nutr.* 2006, *136*, 1150 – 1155.

[21] Saito, Y., Shiga, A., Yoshida, Y., Furuhashi, T. *et al*., Effects of novel gaseous antioxidative system containing a rosemary extract on the oxidation induced by nitrogen dioxide and ultraviolet radiation, *Biosci. Biotechnol. Biochem.* 2004, *68*, 781 – 786.

[22] Sharma, S. D., Meeran, S. M., Katiyar, S. K., Dietary grape seed proanthocyanidins inhibit UVB-induced oxidative stress and activation of mitogen-activated protein kinases and nuclear factor-κB signaling in in vivo SKH-1 hairless mice, *Mol. Cancer Ther.* 2007, *6*, 995 – 1005.

[23] Yamakoshi, J., Otsuka, F., Sano, A., Tokutake, S., *et al*., Lightening effect on ultraviolet-induced pigmentation of guinea pig skin by oral administration of a proanthocyanidin-rich extract from grape seeds, *Pigment. Cell. Res.* 2003, *16*, 629 – 638.

[24] Torre, L. C., Barritt, B. H., Quantitative evaluation of rubus fruit anthocyanin pigments, *J. Food Sci.* 1977, *42*, 488 – 490.

[25] Hong, V., Wrolstad, R. E., Use of HPLC separation/photodiode array detection for characterization of anthocyanins, *J. Agric. Food Chem.* 1990, *38*, 708 – 715.

[26] Choi, Y. J., Jeong, Y. J., Lee, Y. J., Kwon, H. M., Kang, Y. H., (–)Epigallocatechin gallate and quercetin enhance survival signaling in response to oxidant-induced human endothelial apoptosis, *J. Nutr.* 2005, *135*, 707 – 713.

[27] Choi, J. S., Choi, Y. J., Shin, S. Y., Li, J., *et al*., Dietary flavonoids differentially reduce oxidized LDL-induced apoptosis in human endothelial cells: Role of MAPK- and JAK/STAT-signaling, *J. Nutr.* 2008, *138*, 983 – 990.

[28] Park, S. H., Park, J. H. Y., Kang, J. S., Kang, Y. H., Involvement of transcription factors in plasma HDL protection against TNF-α-induced vascular cell adhesion molecule-1 expression, *Int. J. Biochem. Cell Biol.* 2003, *35*, 168 – 182.

[29] Bernerd, F., Asselineau, D., An organotypic model of skin to study photodamage and photoprotection in vitro, *J. Am. Acad. Dermatol.* 2008, *58*, S155 – S159.

[30] Afaq, F., Syed, D. N., Malik, A., Hadi, N., *et al*., Delphinidin, an anthocyanidin in pigmented fruits and vegetables, protects human HaCaT keratinocytes and mouse skin against UVB-mediated oxidative stress and apoptosis, *J. Invest. Dermatol.* 2007, *127*, 222 – 232.

[31] Wlaschek, M., Ma, W., Jansen-Dürr, P., Scharffetter-Kochanek, K., Photoaging as a consequence of natural and therapeutic ultraviolet irradiation-studies on PUVA-induced senescence-like growth arrest of human dermal fibroblasts, *Exp. Gerontol.* 2003, *38*, 1265 – 1270.

[32] Vayalil, P. K., Mittal, A., Hara, Y., Elmets, C. A., Katiyar, S. K., Green tea polyphenols prevent ultraviolet light-induced oxidative damage and matrix metalloproteinases expression in mouse skin, *J. Invest. Dermatol.* 2004, *122*, 1480 – 1487.

[33] Mantena, S. K., Meeran, S. M., Elmets, C. A., Katiyar, S. K., Orally administered green tea polyphenols prevent ultraviolet radiation-induced skin cancer in mice through activation of cytotoxic T cells and inhibition of angiogenesis in tumors, *J. Nutr.* 2005, *135*, 2871 – 2877.

[34] Cimino, F., Cristani, M., Saija, A., Bonina, F. P., Virgili, F., Protective effects of a red orange extract on UVB-induced damage in human keratinocytes, *Biofactors* 2007, *30*, 129 – 138.

[35] Cooper, S. J., Bowden, G. T., Ultraviolet B regulation of transcription factor families: Roles of nuclear factor-κB (NF-κB) and activator protein-1 (AP-1) in UVB-induced skin carcinogenesis, *Curr. Cancer Drug Targets* 2007, *7*, 325 – 334.

[36] El-Mahdy, M. A., Zhu, Q., Wang, Q. E., Wani, G., *et al*., Naringenin protects HaCaT human keratinocytes against UVB-induced apoptosis and enhances the removal of cyclobutane pyrimidine dimers from the genome, *Photochem. Photobiol.* 2008, *84*, 307 – 316.

[37] Wei, H., Saladi, R., Lu, Y., Wang, Y., *et al*., Isoflavone genistein: Photoprotection and clinical implications in dermatology, *J. Nutr.* 2003, *133*, 3811S – 9S.

[38] Huang, C., Zhang, D., Li, J., Tong, Q., Stoner, G. D., Differential inhibition of UV-induced activation of NF kappa B and AP-1 by extracts from black raspberries, strawberries, and blueberries, *Nutr. Cancer* 2007, *58*, 205 – 212.

[39] Afaq, F., Ahmad, N., Mukhtar, H., Suppression of UVB-induced phosphorylation of mitogen-activated protein kinases and nuclear factor kappa B by green tea polyphenol in SKH-1 hairless mice, *Oncogene* 2003, *22*, 9254 – 9264.

[40] Li, L. H., Wu, L. J., Tashiro, S. I., Onodera, S., *et al*., The roles of Akt and MAPK family members in silymarin's protection against UV-induced A375-S2 cell apoptosis, *Int. Immunopharmacol.* 2006, *6*, 190 – 197.

